$AgCuVO_4$: A quasi-one-dimensional $S=\frac{1}{2}$ chain compound

A. Möller,[1,*] M. Schmitt,[2] W. Schnelle,[2] T. Förster,[2] and H. Rosner[2]
[1]*Institut für Anorganische Chemie, Universität zu Köln, Greinstr. 6, 50939 Köln, Germany*
[2]*Max-Planck-Institut für Chemische Physik fester Stoffe, Nöthnitzer Str. 40, 01187 Dresden, Germany*
(Received 5 June 2009; published 9 September 2009)

We present a joint experimental and computational study of the recently synthesized spin 1/2 system silver-copper-orthovanadate $AgCuVO_4$ [A. Möller and J. Jainski, Z. Anorg. Allg. Chem. **634**, 1669 (2008)] exhibiting chains of *trans* corner-sharing $[CuO_4]$ plaquettes. The static magnetic susceptibility and specific heat measurements of $AgCuVO_4$ can be described to a good approximation by the Bonner-Fisher spin-chain model with $J_{intra} \approx 330$ K. Evidence for a Néel-type of order at ~2.5 K is obtained from the specific heat and corroborated by ESR studies. To independently obtain a microscopically based magnetic model, density functional electronic structure calculations were performed. In good agreement with the experimental data, we find pronounced one-dimensional magnetic exchange along the corner-sharing chains with small interchain couplings. The difference between the experimentally observed and the calculated ordering temperature can be assigned to a sizable interchain frustration derived from the calculations.

DOI: 10.1103/PhysRevB.80.125106 PACS number(s): 71.20.−b, 75.30.Et

I. INTRODUCTION

The quest for materials that form quasi-one-dimensional magnetic subunits has evolved into an important part of modern solid-state physics and chemistry over the last one or two decades.[1] Concerning quasi-one-dimensional spin chains, the fundamentally different behavior of systems of even and odd spin numbers has been one of the most spectacular theoretical findings by Haldane already in 1983.[2] In subsequent years it was realized that a large variety of exotic ground states and different unconventional elementary excitations are realized in low-dimensional quantum $S=\frac{1}{2}$ systems, in many cases due to frustration effects. In particular, the ground-state properties of a $S=\frac{1}{2}$ chain with nearest and next-nearest neighbor interactions were calculated by Bursill *et al.*[3] with the result of a spiral spin order, depending sensitively on the ratio of the interaction parameters J_{ij} of the corresponding Heisenberg Hamiltonian

$$\hat{H} = \sum_{\langle ij \rangle} J_{ij} \hat{S}_i \hat{S}_j. \quad (1)$$

On the experimental side, the field of low-dimensional quantum magnetism has recently seen a considerable impetus from another subject of research activity, namely, multiferroicity.[4] Naito *et al.*[5] found that the spiral spin order of $S=\frac{1}{2}$ chains in $LiCuVO_4$ is able to induce a ferroelectric polarization at temperatures below ≈2.4 K. A similar behavior has been observed for $LiCu_2O_2$.[6] The appropriate magnetic model[7–10] and the theoretical description of this phenomenon has been controversially discussed in the literature recently, from both a phenomenological[11] and microscopical point of view.[12,13]

In order to gain further insight into the phenomena and mechanisms at work, it is important to study similar systems with comparable characteristics. From a structural point $S=\frac{1}{2}$ chains of interlinked $[CuO_4]$ plaquettes may connect via edges or corners. Whereas the latter systems show typically antiferromagnetic nearest-neighbor (NN) couplings, the edge-shared systems [i.e., $LiCuVO_4$ (Ref. 14) and $LiCu_2O_2$ (Ref. 8)] exhibit either ferro- or antiferromagnetic NN couplings according to their Cu-O-Cu bond angles close to 90° in agreement with the Goodenough-Kanamori-Anderson rules.[15] A further structural feature is whether the $[CuO_4]$ plaquettes of the chain are all orientated in a coplanar or corrugated/buckled fashion. This will significantly affect the intrachain exchange parameters J_{intra} as well. For example, for the (planar) chain system Sr_2CuO_3 of corner-sharing $[CuO_4]$ plaquettes one finds a pronounced contribution J_{NNN} from next-nearest neighbors (NNNs) with $J_{NN}/J_{NNN} \approx 25$.[16]

Furthermore, the influence of interchain interactions needs to be considered and evaluated especially in the very low-temperature regime. Thereby, a classification of the one-dimensional systems regarding their magnetic properties may be achieved, e.g., spin-Peierls transition (dimerized model) or magnetically ordered exhibiting either classical Néel or spiral spin order, respectively.

In this paper, we present a combined experimental and theoretical study of the $S=\frac{1}{2}$ chain compound $AgCuVO_4$ (Fig. 1), which was synthesized recently.[17] A classification of this system only based on its crystal structure is far from obvious: whereas the $[CuO_4]$ plaquettes in $AgCuVO_4$ form corner-shared chains, the Cu-O-Cu bond angles are rather close to the typical angles in edge-shared cuprate chains. Our combined approach shows consistently that $AgCuVO_4$ can be described as a quasi-one-dimensional $S=\frac{1}{2}$ NN-only Heisenberg chain in very good approximation.

II. METHODS

Powder samples of $AgCuVO_4$ were synthesized by solid-state reactions of CuO and α-$AgVO_3$ (obtained from Ag_2O and V_2O_5) at 700 K in alumina crucibles in air. Powder pellets were pressed using a self-made molding press and sintered for several days at 700 K. These samples were then used for measurements of the physical properties.[33] The phase purity of all samples was checked by powder x-ray diffraction. Low temperature x-ray diffraction patterns were

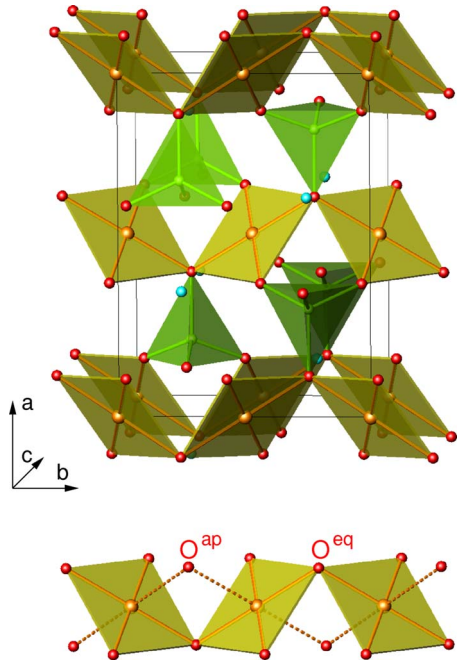

FIG. 1. (Color online) Top: crystal structure of $AgCuVO_4$. Green: $[VO_4]$ tetrahedra. Yellow: $[CuO_4]$ distorted square-planar entities. Light blue: Ag atoms. Bottom: chainlike connectivity of the $[CuO_4]$ units in $AgCuVO_4$. [Cu-O^{eq} (bold lines), Cu-O^{ap} (dotted lines)].

measured on a Stoe & Cie. diffractometer equipped with a closed-cycle Helium cryostat (Lake Shore) using Cu $K\alpha$ radiation between 20 and 293 K. All measured diffraction patterns could be indexed and refined in the space group *Pnma* discussed below, revealing no structural transition in the investigated range.

The static magnetic susceptibility of $AgCuVO_4$ was measured in external magnetic fields of 0.1 and 0.5 T in field-cooled (fc) and zero-field-cooled (zfc) mode [superconducting quantum interference device (SQUID) magnetometer; MPMS, Quantum Design].

The electron spin resonance (ESR) measurements were performed at *X*-band frequencies ($f=9.4$ GHz) using a standard spectrometer together with a He-flow cryostat that allows to vary the temperature from 2.6 to 300 K. ESR probes the absorbed power P of a transversal magnetic microwave field as a function of a static and external magnetic field B. To improve the signal-to-noise ratio, we used a lock-in technique by modulating the static field, which yields the derivative of the resonance signal dP/dB.

The heat capacity was determined on the same sample by a relaxation-type method ($m \approx 11$ mg; PPMS, Quantum Design) in external magnetic fields of 0, 3, 6, and 9 T.

For the electronic structure calculations the full-potential local-orbital scheme FPLO (version: fplo7.00–28) within the local (spin) density approximation [L(S)DA] was used.[18] In the scalar relativistic calculations the exchange and correlation potential of Perdew and Wang was chosen.[19] To consider the strong electron correlations for the Cu^{2+} ($3d^9$) configuration, we use the LSDA+U (Ref. 20) approximation varying U_d in the physically relevant range 6–8.5 eV. The LDA results were mapped onto an effective tight-binding (TB) model and subsequently to a Hubbard and a Heisenberg model.

III. CRYSTAL STRUCTURE

Figure 1 shows a perspective view of the crystal structure of $AgCuVO_4$. The compound crystallizes in the orthorhombic space group *Pnma* with lattice parameters $a=9.255(1)$ Å, $b=6.778(1)$ Å, and $c=5.401(1)$ Å, as determined by single-crystal x-ray diffraction at room temperature.[17] Isolated $[VO_4]$ tetrahedra (containing "nonmagnetic" V^{5+}) are connected to the Cu^{2+} ions as bridging complex ions within the chain as well as between neighboring chains of *trans* corner-sharing $[CuO_4]$ plaquette entities along the b axis. These chains are furthermore separated from each other by isolated nonmagnetic Ag^+ ions, also shown in Fig. 1. A more detailed description of the crystal structure is given by Möller and Jainski.[17]

The magnetic Cu^{2+} ions ($S=\frac{1}{2}$) are coordinated by four oxygen atoms in a square-planar fashion with a typical average Cu-O^{eq} distance of 1.995 Å, whereas the distance to the two apical oxygen atoms (O^{ap}), designated by dotted lines in Fig. 1, is 2.511(4) Å. Considering the elongated octahedral coordination of Cu^{2+} a $d_{x^2-y^2}$ ground-state character can be assumed. The bridging angle $\angle$(Cu-O^{eq}-Cu) within the chains is 113.0(2)°, indicative of predominantly antiferromagnetic interactions of the spins according to the Goodenough-Kanamori-Anderson rules.[15] Although Fig. 1 suggests an edge-sharing connectivity within the chains, the effective exchange via the apical oxygen atom (O^{ap}) is almost negligible, since the related d_{z^2} is fully occupied. Any superexchange via O^{ap} would be expected to give a ferromagnetic coupling in relation to the bridging angle (Cu-O^{ap}-Cu) of 85°. Therefore, one might consider this system as a quasi-one-dimensional $S=\frac{1}{2}$ antiferromagnet build of *trans* corner-sharing $[CuO_4]$ plaquettes. However, it should be noted that $AgCuVO_4$ is not isotypic with $LiCuVO_4$ which contains edge-sharing $[CuO_4]$ plaquette entities. Thus, distinct differences with respect to the magnetic interaction pathways associated with the Cu^{2+} $d_{x^2-y^2}$ ground state occur.

IV. RESULTS AND DISCUSSION

A. Magnetic susceptibility

The temperature dependence of the static magnetic susceptibility measured in a field of 0.1 T in fc mode is plotted in Fig. 2. The broad maximum in $\chi(T)$ at around 200 K is a typical feature of a low-dimensional magnetic system. Toward lower temperatures, below approximately 50 K, a sharp upturn in the form of a "Curie-tail" occurs, which most probably originates from paramagnetic impurities. Measurements at 0.1 and 0.5 T showed identical behavior in fc and zfc mode (not shown here). At higher temperatures, the magnetic susceptibility $\chi(T)$ can be described according to the isotropic one-dimensional $S=\frac{1}{2}$ model of Bonner and Fisher[21] using the spin-spin Hamiltonian in the form of $\hat{H}=J_{\text{intra}}\Sigma\hat{S}_i\hat{S}_{1+i}$. A magnetic coupling constant of J^{χ}_{intra}

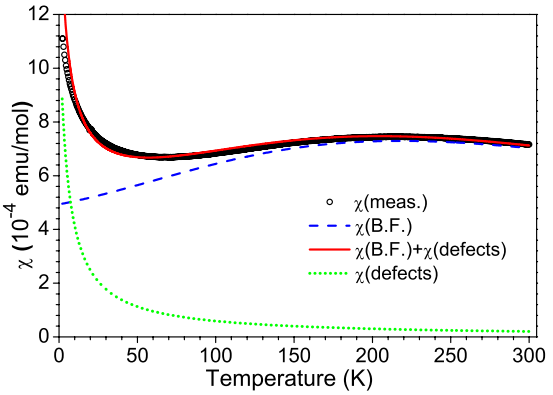

FIG. 2. (Color online) Temperature dependence of the static magnetic susceptibility of $AgCuVO_4$ (0.1 T, fc), black circles. χ(B.F.) gives the result for an isotropic chain (Bonner-Fisher model, dashed blue line) and χ (defects) presents the impurity contribution, dotted green line. The total fit is given by the red line.

≈ 335 K is derived for $AgCuVO_4$ (see dashed line in Fig. 2). We used a typical constant value for the g factor ($g_{\text{average}} \approx 2.10$) for the determination of J^{χ}_{intra} within the isotropic Heisenberg model. At low temperatures the magnetic contribution of defects becomes evident. Including 1.5% paramagnetic $S=\frac{1}{2}$ impurities (defects, dotted line) with a Weiss temperature of $\Theta_{\text{imp}} \approx -5$ K we obtain a fit in good agreement with the experimental data for the temperature range from 10 to 300 K (red line of Fig. 2).

The effective antiferromagnetic coupling indicates a dominant $d_{x^2-y^2}$ ground-state character of the Cu^{2+} ion in agreement with a superexchange path via the bridging oxygen atoms O^{eq} with an angle of 113° in this case. Of course, this highly oversimplified picture relating to structural arguments calls for a more detailed analysis based on specific heat, ESR measurements and LDA calculations.

B. Electron spin resonance

Figure 3 shows a typical ESR signal at $T=10$ K (inset) and the temperature behavior of the line width (top panel) for $AgCuVO_4$. At temperatures $T>4$ K we observe a well defined signal which could be nicely fitted with a single Lorentzian line (red line in inset) providing the ESR parameters line width ΔB and g factor ($g=h\nu/\mu_B B_{\text{res}}$, B_{res} resonance field). Below 4 K an additional signal with a twice larger line width and nearly the same resonance field occurs. This second signal might be related to the anisotropy of the ESR parameters, but could also originate from impurities or indicate a resonance mode resulting from an antiferromagnetic ordered state.

In the two lower panels in Fig. 3 the temperature behavior of the ESR intensity and the measured g factor is shown. The observed g values of $\approx 2.17(1)$ are typical for Cu^{2+} in a distorted octahedral environment and in fair agreement with the static susceptibility fitted by the Bonner-Fisher model. Above 10 K the intensity follows the magnetic susceptibility $\chi(T)$ (see Fig. 2) reproducing the broad minimum around 40 K. Below $T=4$ K the ESR intensity reduces rapidly toward lower temperatures indicating a magnetic ordering

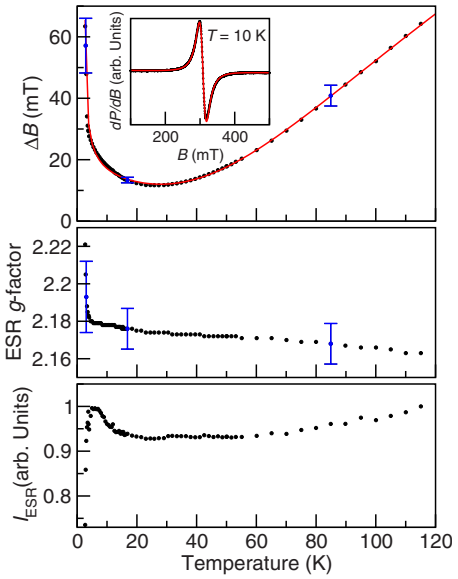

FIG. 3. (Color online) The inset shows a typical ESR signal (black circles) with a Lorentzian fit (red line) given. The temperature dependence of the signals line width (black circles) and a fit with Eq. (2) to the data (red line) is shown for $AgCuVO_4$ in the top main panel. The two lower panels show the temperature dependence of the g factor (middle) and the intensity of the ESR signal (bottom panel) for $AgCuVO_4$.

below 4 K. A similar behavior above T_N is observed in the spin chain compound $CuSiO_3$.[22]

The divergence of the g factor and the line width at low temperatures also indicate a magnetic phase transition below 4 K. The temperature dependence of the line width $\Delta B(T)$ is comparable with that of $LiCuVO_4$ (Ref. 23) and $CuGeO_3$ (Ref. 24) showing a pronounced minimum between 10 and 40 K. We fitted $\Delta B(T)$ with a classical critical divergence at T_N [first term in Eq. (2) below] and an empirical expression for the high-temperature part.[24][second term in Eq. (2)]

$$\Delta B = C\left(\frac{T}{T_N} - 1\right)^{-p} + \Delta B(\infty)\exp\left(-\frac{C_1}{T + C_2}\right), \qquad (2)$$

C, p, T_N, $\Delta B(\infty)$, C_1, and C_2 are treated as six fitting parameters. Table I summarizes the fit results.

The fit results on the first term in Eq. (2) depend only weakly on the parameters of the second term and vice versa. This holds especially for T_N. The influence of the other parameters is included in the uncertainty displayed in Table I.

C_1 is related to the order of magnitude of the isotropic exchange constant, because the parameter indicates the transition from the strongly correlated one-dimensional regime at

TABLE I. Fit parameters according to Eq. (2) for the line width of the ESR signals for $AgCuVO_4$

C (mT)	p	T_N (K)	$\Delta B(\infty)$ (mT)	C_1 (K)	C_2 (K)
35 ± 0.7	0.35 ± 0.05	2.5 ± 0.2	294 ± 50	199 ± 30	6 ± 5

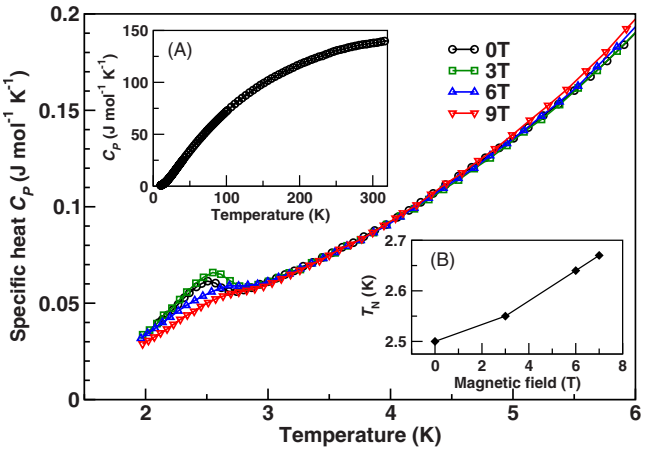

FIG. 4. (Color online) Temperature dependence of the specific heat of $AgCuVO_4$ for different magnetic fields. Inset (a): large temperature range in zero field. Inset (b): field dependence of the Néel temperature.

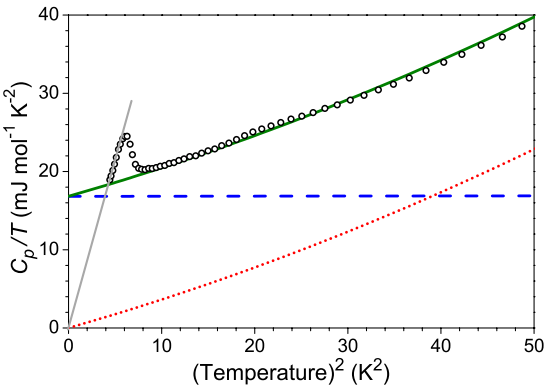

FIG. 5. (Color online) Magnetic heat capacity C_P/T at zero field versus T^2 (black circles) for $AgCuVO_4$ including the fit to Eq. (3) (green line) as well as C_m/T (dashed blue line) and C_l/T (dotted red line). The gray line presents a linear fit below T_N, see text.

low temperatures $T \ll J_{\text{intra}}$ to the purely paramagnetic regime $T \gg J_{\text{intra}}$. C_2 indicates the influence of the low-temperature phase transition (long-range magnetically ordered phase) on the line broadening. It is necessary to recall that this purely empirical parametrization has no underlying microscopic picture. Nevertheless, the ESR corroborates the antiferromagnetic ground state and the onset of long-range order setting in at ≈ 2.5 K (see Sec. IV C on the specific heat capacity below).

C. Specific heat capacity

Inset (A) of Fig. 4 shows the measured specific heat capacity, $C_p(T)$, in zero field for $AgCuVO_4$ below 320 K. The field dependence of $C_p(T)$ is given in the main panel of Fig. 4. Below 3 K an anomaly is clearly visible in lower fields, which broadens and smears out with increasing field. The field dependence indicates that this effect can be attributed to an antiferromagnetically ordered ground state. The shift in the Néel temperature with increasing field from 2.5 to almost 2.7 K is shown in the inset (B) of Fig. 4. We have fitted $C_p(T)/T$ versus T^2 below 10 K (Fig. 5) to Eq. (3) in order to obtain the coefficients (γ and β_1) related to the magnetic $[C_m(T)]$ and lattice $[C_l(T)$; harmonic lattice approximation] part of the specific heat.

$$C_p(T)/T = \gamma + \beta_1 T^2 + \beta_2 T^4. \tag{3}$$

The lattice contribution (phonons) is associated with $\beta_1 = 0.34(5)$ mJ mol^{-1} K^{-4} and allows an estimate of the Debye temperature $\Theta_D = (12\pi n N_A k_B / 5\beta_1)^{1/3} \approx 342$ K, a typical value for $^1_\infty[CuO_{4/2}]$ compounds with edge-sharing connectivity.[25] The value of $\beta_2 = 0.00234(4)$ mJ mol^{-1} K^{-6} is of the expected magnitude ($\sim 1\% \beta_1$). The magnetic part of the specific heat is presented by $\gamma = C_m/T$. $C_m(T)/T$ is found to be almost constant at low temperatures for an isotropic $S = 1/2$ chain and related to the magnetic exchange parameter, $J_{\text{intra}} = 2N_A k_B / (3C_p^{(T \to 0)}/T)$.[26] With $\gamma = 16.9(1)$ mJ mol^{-1} K^{-2} we find within the Heisenberg model $J_{\text{intra}}^{C_p}$ of about 330 ± 10 K in excellent agreement with the value derived from the fit to the susceptibility data.

The long-range order setting in below 3 K occurs from interchain couplings and the Néel temperature, T_N, associated with this transition can be used to estimate the exchange parameter $J_{\text{inter}}^{C_p}$ of ≈ 0.75 K from Eq. (4) (Ref. 27)

$$J_{\text{inter}} = T_N / [1.28 \sqrt{\ln(5.8 J_{\text{intra}}/T_N)}]. \tag{4}$$

In principle the same result is obtained from a more recent theoretical approach[28] to estimate the interchain coupling from T_N. Here, the intrachain coupling parameters J_{intra} derived from $C_p(T)$ and $\chi(T)$ data are not only consistent but almost identical. Furthermore, J_{intra} is found to be about 440 times larger than J_{inter}. Therefore, $AgCuVO_4$ can be regarded as a quasi-one-dimensional $S = \frac{1}{2}$ system at $T \gg 3$ K. For a more detailed analysis and evaluation of J_{inter} in this case see Sec. IV D on the electronic structure below.

In Fig. 5 a linear fit below T_N ($T^2 < 5.5$ K) is included. The extrapolated intersection with the origin is in agreement with the insulating properties of $AgCuVO_4$ and reveals the magnon contribution to the total specific heat capacity, C_p, which follows approximately a T^3 law typical for an antiferromagnet.

D. Electronic structure

To gain microscopic insight into the electronic and magnetic properties of the system we carried out band structure calculations based on density functional theory (DFT) and subsequent model calculations.

In Fig. 6 the obtained density of states (DOS) of the valence states with a bandwidth of about 6 eV is shown. This bandwidth is rather typical compared with other cuprates revealing a chain-type of structural feature like $CuGeO_3$ (Ref. 29) or Sr_2CuO_3.[16] The valence band is dominated by Ag, Cu, and O states. The quite narrow Ag $4d$ contribution between -2 eV and -0.5 eV indicates a Ag^+ cation. For Cu and V the calculations yield magnetic Cu^{2+} and nonmagnetic V^{5+} as could be expected from the crystal structure in terms of their coordination spheres (see Fig. 1): Cu and O form strongly distorted $[CuO_6]$ octrahedra with considerably shorter Cu-O^{eq} bonds in the equatorial plane leading to the charac-

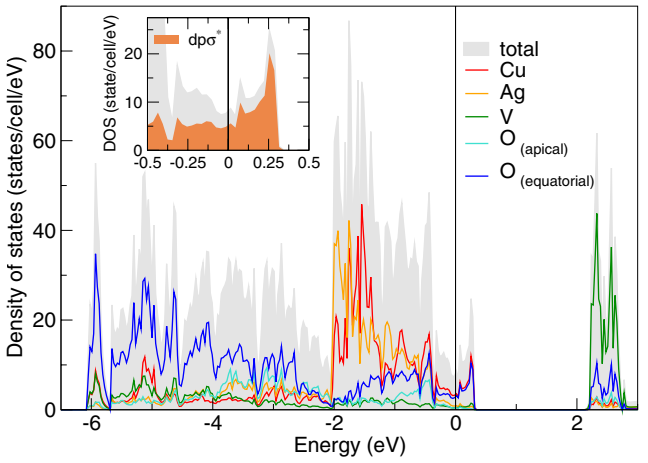

FIG. 6. (Color online) Calculated total and atom resolved density of states for AgCuVO$_4$. The Fermi level is at zero energy. Inset: orbital-resolved density of states for the $dp\sigma^*$ states of the antibonding half-filled band.

teristic [CuO$_4$] plaquettes, whereas the nonmagnetic V^{5+} is tetrahedrally coordinated, [VO$_4$]. Magnetically active V^{4+} usually appears in drastically distorted coordination spheres (e.g., square pyramidal).

As a consequence of the Cu^{2+} state the antibonding Cu-O dpσ^* states of the system are half filled. Corresponding to the 4 Cu per unit cell, four half-filled bands cross the Fermi energy ε_F (see Fig. 7) in our LDA calculation. This metallic solution is in contradiction to the insulating character of the compound concluded from the red color of the crystals and a well-known shortcoming of the LDA calculations. As LDA underestimates the strong correlations of the Cu^{2+} ($3d^9$) configuration, these missing correlations can be taken into account by mapping the relevant LDA bands onto a TB model and subsequently onto a Hubbard and Heisenberg model. Alternatively the strong Coulomb repulsion in the Cu $3d$ shell can be considered explicitly in a mean-field-like approach using the LSDA+U scheme.

In many cuprates the antibonding dpσ^* states are well separated from the lower-lying valence states, while in AgCuVO$_4$ these states overlap with the lower-lying part of the valence due to a sizable admixture of other orbitals. The inset of Fig. 6 shows the orbital-resolved DOS of the Cu-O dpσ^* states in comparison with the total DOS. In the region between ε_F and 0.25 eV the dpσ^* states clearly dominate the antibonding bands, whereas from ε_F to −0.5 eV contributions from other orbitals increases notably. Accordingly, the hybridization with lower-lying parts of the valence band is also visible in the upper panel of Fig. 7 where the band characters of the dpσ^* states spread out to lower energies (mainly around Γ and X).

The sizable admixture of other valence states to the antibonding bands that are responsible for the magnetic interactions in the system impedes a straightforward mapping to an effective one-band TB model using a least-square fit procedure. The ambiguousness in the selection of the relevant bands, especially between Γ and X and Γ and Z, respectively, can be removed applying the Wannier function technique (see Fig. 9). The resulting leading transfer terms for both

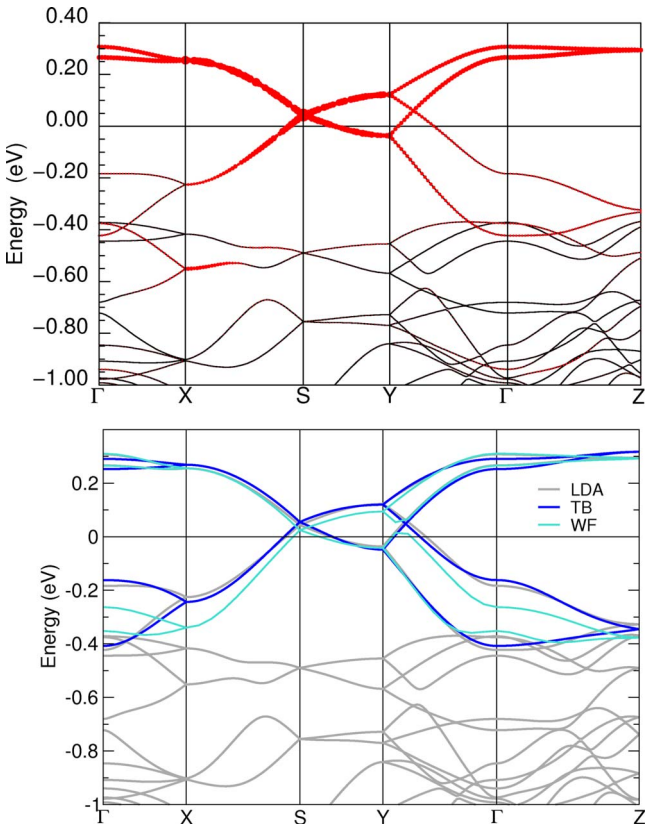

FIG. 7. (Color online) LDA band structure of AgCuVO$_4$ overlaid with the band characters of the antibonding $dp\sigma^*$ states (upper panel) and with the bands from a direct tight-binding (TB) fit and from a Wannier function (WF) based mapping (lower panel).

approaches are sketched in Fig. 8 and the values are given in Table II. The corresponding bands are highlighted in Fig. 7 (lower panel) on top of the LDA band structure. It can be clearly seen that in the upper part the least square TB fit and the Wannier function derived bands nearly coincide, while for the lower-lying region with stronger admixture (see inset Fig. 6), both approaches show sizable deviations. This is mostly reflected in the leading NN transfer integral t_1, whereas the much smaller coupling to further neighbors are

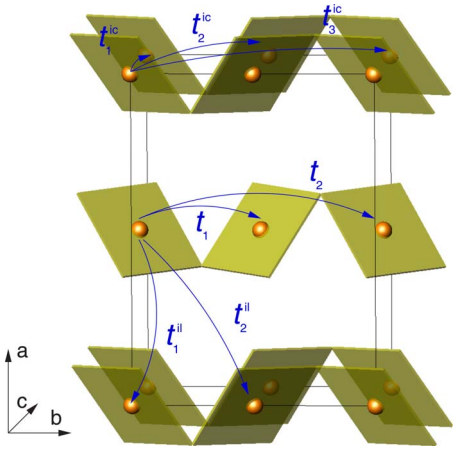

FIG. 8. (Color online) Sketch of the TB model for AgCuVO$_4$

TABLE II. Leading coupling terms for $AgCuVO_4$ from TB and Wannier function (WF) approach.

t_i/meV	t_1	t_2	t_1^{ic}	t_2^{ic}	t_3^{ic}	t_1^{il}	t_2^{il}
t_i(TB)	−145	2	17	7	6/−19	−16	−11/0
t_i(WF)	−157	0	18	6	5/−20	−13	−10/3

mostly unaffected. On the other hand, the good agreement between both methods justifies the application of an effective one-band picture.

From our mapping, we obtain a clear physical picture for the relevant interactions in the system: we find weakly interacting chains along the *b* direction with essentially only NN coupling t_1 (see Table II). Consistent with the Cu-O-Cu bond angle of about 113° this leading transfer is closer to the values for edge-shared chain geometry (e.g., $CuGeO_3$,[29] Cu-O-Cu bond angle of about 99°, $t_1 \approx 175$ meV) than for the couplings of the corner-shared chains (e.g., Sr_2CuO_3,[16] Cu-O-Cu bond angle of 180°, $t_1 \approx 410$ meV). This vicinity to the edge-shared chain compounds raises the question of the relevance of ferromagnetic contributions to the NN exchange J_1. Mapping the TB model via a Hubbard to a Heisenberg model (in the limit of strong correlations and at half-filling) to describe the low-lying magnetic excitations only yields the antiferromagnetic parts $J_i^{AF}=4t_i^2/U_{eff}$ of the total exchanges J_i. The ferromagnetic contributions can be estimated comparing the TB derived exchange J_i^{AF} with the result of LSDA+U calculations for magnetic super cells. Using a standard one-band value $U_{eff}=4$ eV (Ref. 29) we obtain for the NN exchange $J_1^{AF}=23\pm3$ meV (265 ± 35 K).[34] For the calculated range of physically relevant U_d values[35] in the LSDA+U approach we obtain $J_{intra}^{TH}\equiv J_1=24\pm3$ meV (280 ± 35 K). The very good agreement between J_1^{AF} and J_{intra}^{TH} leads us to the conclusion that ferromagnetic contributions to the NN exchange in $AgCuVO_4$ are basically negligible. The choice of U_d is additionally justified by the resulting gap size of $1.5\cdots2$ eV consistent with the red color of the sample and in agreement with measurements of the absorption in the visible part of the electromagnetic spectrum at significantly lower energy for $AgCuVO_4$ in comparison with α-$AgVO_3$ (reported gap of ≈2.3 eV) (Ref. 30) as a reference.

A closer inspection of the effective exchange path by the calculated Wannier functions (see Fig. 9) shows that the interaction does not appear from a coupling via the shared O^{eq} only, but also involves states of the $[VO_4]$ tetrahedra. These contributions are in line with the picture obtained from the orbital resolved DOS (see Fig. 6 and inset) with additional states mixing into the antibonding dpσ^* band.

It is well-known that for ideal one-dimensional chains no magnetic order appears.[31] In our compound, we calculated interchain couplings J_{inter}^{TH} of the order of 1/65 with respect to the NN intrachain exchange $J_1=J_{intra}^{TH}$. The calculated exchange values allow the estimate of the ordering temperature T_N according to Eq. (4).[27] Using $J_1=24$ meV (280 K) and an effective $J_{inter}^{TH}=0.25$ meV (3 K) as an average of the interchain couplings J_1^{ic} and J_3^{ic} in the crystallographic *bc* plane and the interlayer exchanges J_1^{il} and J_2^{il} (see Fig. 8) we obtain a theoretical value $T_N^{TH}=8.6(5)$ K for the Néel temperature.

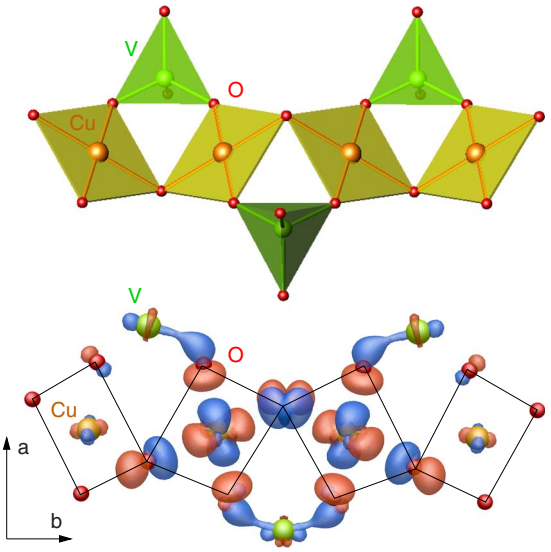

FIG. 9. (Color online) Cu $3d_{x^2-y^2}$ related Wannier functions for a chain segment in $AgCuVO_4$.

Compared to the experimentally observed $T_N=2.5$ K this is a clear overestimate by a factor of ≈3.5. A closer inspection of the further magnetic interactions between chains belonging to different "magnetic layers" separated by a diagonal component along the crystallographic *a* direction (J^{il}, cf. Table II) reveals the frustrating nature of the leading interlayer couplings J_1^{il} and J_2^{il} (compare Fig. 8 and see Fig. 10). Therefore, we can assign the deviation of the calculated and observed T_N to the latter considerable interchain frustration. The situation is comparable to the quasi-one-dimensional model compound Sr_2CuO_3, where a similar suppression of the ordering temperature compared to the calculation appears.[16] The strong influence of frustration on the ordering temperature is especially pronounced for the compound $Sr_2Cu(PO_4)_2$, where the leading interchain couplings $J_\perp$ are fully frustrated.[32] Although the main couplings are comparable to $AgCuVO_4$, the ordering temperature of $Sr_2Cu(PO_4)_2$ is smaller by a factor of about 30. The strong quantum fluctuation in quasi-one-dimensional spin-$\frac{1}{2}$ compounds not only lead to a drastic reduction in the ordering temperature, but

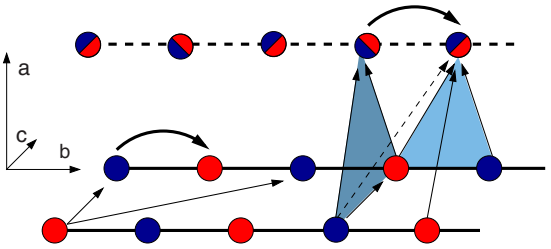

FIG. 10. (Color online) Sketch of the magnetic model for $AgCuVO_4$. The leading interchain exchange terms yield unfrustrated coupling between the chains in the crystallographic *bc* plane, but sizable frustration between the layers (indicated by filled triangles). This is illustrated by the different colors (red, blue) for different spin directions according to the antiferromagnetic nature of the relevant exchange couplings.

also to a small ordered moment. Using the same exchange parameters as for the calculation for T_N we predict an ordering moment of about 0.15 μ_B (Eq. 7 in Ref. 27). In conclusion, our band structure calculations provide us with a picture (see Fig. 10) of quasi-one-dimensional NN Heisenberg chains with small interchain couplings where the in-plane couplings J^{ic} support AFM order, whereas sizable interlayer frustration J^{il} impedes AFM.

V. SUMMARY AND CONCLUSIONS

We have presented measurements of the static magnetic susceptibility and the specific heat capacity, which evidence the pronounced one-dimensional magnetic properties of $AgCuVO_4$ related to structural features and to the $d_{x^2-y^2}$ ground-state character of the Cu^{2+} ion. Within the isotropic exchange model for a Heisenberg system $J_{intra} \approx 330$ K has been derived from the experimental data. Furthermore, weak interchain coupling is evident from specific heat capacity and ESR measurements leading to a magnetically ordered state at $T_N=2.5$ K. In order to gain insight into the magnetic interactions on a microscopic basis we performed full-potential electronic structure calculations. Subsequently derived Heisenberg models based on Wannier functions and LSDA $+U$ calculations confirm the quasi-one-dimensional behavior. We found the main exchange along the chain $J_{intra}^{TH} = 280 \pm 35$ K in good agreement with the thermodynamic measurements and several small interchain couplings leading to an estimate for the antiferromagnetic ordering temperature $T_N^{TH} \sim 8.6$ K. From the magnetic model (see Fig. 10) the overestimate of T_N^{TH} by a factor of 3.5 compared to the experimental observed ordering temperature can be attributed to frustrated interchain couplings along the crystallographic a direction. All interchain couplings are fairly weak and according to our experimental data and calculations neither spiral order and subsequent multiferroic behavior nor a spin-Peierls transition is expected for $AgCuVO_4$. Moreover, this compound with effective NN couplings of the order of room temperature can be classified as "in between" edge- and corner-shared chains and might serve as a good candidate to study the characteristic properties of a one-dimensional $S=\frac{1}{2}$ Heisenberg system also by other complementary methods in temperature ranges that are experimentally easier accessible. In particular, single crystals are highly desirable for further investigation of the thermal transport and expansion behavior as well as for studies of the ordered magnetic moment and the magnon dispersion by neutron diffraction.

ACKNOWLEDGMENTS

This work was supported by the DFG through Grant No. SFB 608. The authors would like to thank Judith Jainski for the sample preparation, Oleg Janson, Jörg Sichelschmidt, and John A. Mydosh for valuable discussions, and U. Nitzsche for the use of the computational facilities at the IFW Dresden.

*Present address: Department of Chemistry and Texas Center for Superconductivity, University of Houston, Houston, Texas 77204-5003, USA.

[1] E. Dagotto and T. M. Rice, Science **271**, 618 (1996).
[2] F. D. M. Haldane, Phys. Rev. Lett. **50**, 1153 (1983).
[3] R. J. Bursill, G. A. Gehring, D. J. J. Farnell, J. B. Parkinson, C. Zeng, and T. Xiang, J. Phys.: Condens. Matter **7**, 8605 (1995).
[4] F. Schrettle, S. Krohns, P. Lunkenheimer, J. Hemberger, N. Büttgen, H.-A. Krug von Nidda, A. V. Prokofiev, and A. Loidl, Phys. Rev. B **77**, 144101 (2008).
[5] Y. Naito, K. Sato, Y. Yasui, Yu. Kobayashi, Yo. Kobayashi, and M. Sato, J. Phys. Soc. Jpn. **76**, 023708 (2007).
[6] S. Park, Y. J. Choi, C. L. Zhang, and S.-W. Cheong, Phys. Rev. Lett. **98**, 057601 (2007).
[7] T. Masuda, A. Zheludev, A. Bush, M. Markina, and A. Vasiliev, Phys. Rev. Lett. **92**, 177201 (2004).
[8] A. A. Gippius, E. N. Morozova, A. S. Moskvin, A. V. Zalessky, A. A. Bush, M. Baenitz, H. Rosner, and S.-L. Drechsler, Phys. Rev. B **70**, 020406(R) (2004).
[9] S.-L. Drechsler, J. Malek, J. Richter, A. S. Moskvin, A. A. Gippius, and H. Rosner, Phys. Rev. Lett. **94**, 039705 (2005).
[10] T. Masuda, A. Zheludev, A. Bush, M. Markina, and A. Vasiliev, Phys. Rev. Lett. **94**, 039706 (2005).
[11] M. Mostovoy, Phys. Rev. Lett. **96**, 067601 (2006); M. Kenzelmann and A. B. Harris, *ibid.* **100**, 089701 (2008); M. Mostovoy, *ibid.* **100**, 089702 (2008).
[12] H. Katsura, N. Nagaosa, and A. V. Balatsky, Phys. Rev. Lett. **95**, 057205 (2005).
[13] I. A. Sergienko and E. Dagotto, Phys. Rev. B **73**, 094434 (2006).
[14] M. Enderle, C. Mukherjee, B. Fåk, R. K. Kremer, J.-M. Broto, H. Rosner, S.-L. Drechsler, J. Richter, J. Malek, A. Prokofiev, W. Assmus, S. Pujol, J.-L. Raggazzoni, H. Rakoto, M. Rheinstädter, and H. M. Rønnow, EPL **70**, 237 (2005).
[15] J. B. Goodenough, *Magnetism and the Chemical Bond* (Wiley, New York, 1963).
[16] H. Rosner, H. Eschrig, R. Hayn, S.-L. Drechsler, and J. Malek, Phys. Rev. B **56**, 3402 (1997).
[17] A. Möller and J. Jainski, Z. Anorg. Allg. Chem. **634**, 1669 (2008).
[18] K. Koepernik and H. Eschrig, Phys. Rev. B **59**, 1743 (1999).
[19] J. P. Perdew and Y. Wang, Phys. Rev. B **45**, 13244 (1992).
[20] H. Eschrig, K. Koepernik, and I. Chaplygin, J. Solid State Chem. **176**, 482 (2003).
[21] J. C. Bonner and M. E. Fisher, Phys. Rev. **135**, A640 (1964).
[22] J. Sichelschmidt, M. Baenitz, C. Geibel, F. Steglich, A. Loidl, and H. H. Otto, Appl. Magn. Reson. **23**, 75 (2002).
[23] H.-A. Krug von Nidda, L. E. Svistov, M. V. Eremin, R. M. Eremina, A. Loidl, V. Kataev, A. Validov, A. Prokofiev, and W. Aßmus, Phys. Rev. B **65**, 134445 (2002).
[24] R. M. Eremina, M. V. Eremin, V. N. Glazkov, H.-A. Krug von Nidda, and A. Loidl, Phys. Rev. B **68**, 014417 (2003).
[25] S.-L. Drechsler, J. Richter, A. A. Gippius, A. Vasiliev, A. A. Bush, A. S. Moskvin, J. Málek, Y. Prots, W. Schnelle, and H. Rosner, EPL **73**, 83 (2006).

[26] D. C. Johnston, R. K. Kremer, M. Troyer, X. Wang, A. Klümper, S. L. Bud'ko, A. F. Panchula, and P. C. Canfield, Phys. Rev. B **61**, 9558 (2000).
[27] H. J. Schulz, Phys. Rev. Lett. **77**, 2790 (1996).
[28] V. Yu. Irkhin and A. A. Katanin, Phys. Rev. B **61**, 6757 (2000).
[29] H. Rosner, S.-L. Drechsler, K. Koepernik, R. Hayn, and H. Eschrig, Phys. Rev. B **63**, 073104 (2001).
[30] R. Konta, H. Kato, H. Kobayashi, and A. Kudo, Phys. Chem. Chem. Phys. **5**, 3061 (2003).
[31] N. D. Mermin and H. Wagner, Phys. Rev. Lett. **17**, 1133 (1966).
[32] M. D. Johannes, J. Richter, S.-L. Drechsler, and H. Rosner, Phys. Rev. B **74**, 174435 (2006).
[33] Unfortunately, single crystals of a suitable size for the thermodynamic measurements could not be obtained so far. Further attempts to grow single crystals are in progress.
[34] The error is estimated from the difference of the least-square fit and the Wannier function approach for the TB model.
[35] Within the range of $U=6\ldots8.5$ eV we obtain agreement with the experimentally reported exchange integrals for a large number of edge- and corner-shared cuprate.